

Optimization of Oxidation Temperature for Commercially Pure Titanium to Achieve Improved Corrosion Resistance

Rajesh Bansal, J.K. Singh, Vakil Singh, D.D.N. Singh, and Parimal Das

(Submitted June 28, 2016; in revised form September 17, 2016; published online February 21, 2017)

Thermal oxidation of commercially pure titanium (cp-Ti) was carried out at different temperatures, ranging from 200 to 900 °C to achieve optimum corrosion resistance of the thermally treated surface in simulated body fluid. Scanning electron microscopy, x-ray diffraction, Raman spectroscopy and electrochemical impedance spectroscopy techniques were used to characterize the oxides and assess their protective properties exposed in the test electrolyte. Maximum resistance toward corrosion was observed for samples oxidized at 500 °C. This was attributed to the formation of a composite layer of oxides at this temperature comprising Ti₂O₃ (titanium sesquioxide), anatase and rutile phases of TiO₂ on the surface of cp-Ti. Formation of an intact and pore-free oxide-substrate interface also improved its corrosion resistance.

Keywords corrosion, cp-titanium, dental implant, electrochemical impedance, titanium oxide, XRD Raman spectroscopy

1. Introduction

Owing to good mechanical properties, chemical stability and biocompatibility, titanium metal and its alloys are extensively used for dental and orthopedic implants, auricular episthesis and bone-anchored hearing aids (Ref 1-4). Titanium metal and their alloys have an inherent property of forming a thin amorphous and/or poorly crystallized oxide layer on their surface. These oxides are primarily composed of TiO₂ (titania) with small proportion of titanium (III) oxide (also known as titanium sesquioxide with chemical formula Ti₂O₃) and titanium oxide (TiO). The properties of the implants are governed by the nature of oxides formed on the metal surface, which differ considerably from that of the bulk material. However, these films are not stable in vivo and can easily be removed even by brushing against soft tissue (Ref 5-7).

Interface between bone and implant can be envisioned as a composite, formed from interaction between body cells and surface layer of the material. Thus, there is definite scope for altering the nature of surface oxide film to achieve improved interaction between cells/body fluid and surface of implant. This interaction is crucial for the development of an initial stable interface and prolonged success of the implant. In order to achieve the aforesaid mechanical, electrochemical and biological properties of titanium-based implants, various surface modification techniques have been used to change the

nature of the oxide film present on their surface. Titanium has high affinity for oxygen and forms different types of oxide films, which increase in thickness in oxidizing environments. This reaction is catalyzed by heat input, oxidizing environments, electrochemical anodization, acid treatment, thermal oxidation, sol-gel oxidation and plasma spray (Ref 8-13). Out of these techniques, thermal oxidation is considered the most economical and commercially viable process. Gemelli et al. (Ref 14) studied the effect of thermal treatment on the nature of oxide film formed on titanium metal and reported the formation of adherent film at 600 °C. Feng et al. (Ref 15) investigated the oxidation of commercially pure titanium at 600 °C in air, water-saturated steam, oxygen and reported the formation of rutile phase (TiO₂) in every environment. Gemelli and Camargo (Ref 16) studied oxidation kinetics of commercially pure titanium at temperature range of 300-1000 °C and reported the transformation of room temperature passive film into rutile and anatase forms of TiO₂. Kumar et al. (Ref 17) found a direct correlation between improvements in corrosion resistance of the passive film on cp-Ti with increase in thermal oxidation temperature from 500 to 800 °C. Guleryuz and Cimenoglu (Ref 13) examined the corrosion and wear resistance of thermally oxidized Ti-6Al-4V alloy and reported a significant improvement in the aforesaid properties of the metal. Alloying of 5% silver metal with titanium was observed to improve corrosion resistance of the alloy in artificial saliva solution in comparison with that of cp-Ti (Ref 18). Rutile titanium dioxide (TiO₂) was reported to form on thermally oxidized titanium and provided lowest passive current in seawater (Ref 19). Published literature reveals that majority of the work on thermal oxidation of titanium metal is related to characterization of the resultant oxides in terms of their morphology, nature, hardness, wear resistance and other mechanical properties. Most of the reported literature pertains to results of the higher-temperature oxidation of titanium. The higher-temperature treatment process to develop oxide layers on titanium metal is associated with many draw backs and hampers the long-term performance of implants. Thermal oxidation of titanium above 800 °C provides thick and highly crystalline rutile phase of oxide (Ref 20). This oxide, though imparts improved properties during its initial exposure to human body fluid but suffers spalling due to

Rajesh Bansal, Faculty of Dental Sciences, Institute of Medical Sciences, Banaras Hindu University, Varanasi, India; **J.K. Singh**, Indian Institute of Engineering Science and Technology, Kolkata, India; **Vakil Singh**, Department of Metallurgical Engineering, Indian Institute of Technology, Banaras Hindu University, Varanasi, India; **D.D.N. Singh**, Corrosion and Surface Engineering, National Metallurgical Laboratory, Jamshedpur, India; and **Parimal Das**, Centre of Genetic Disorders, Institute of Sciences, Banaras Hindu University, Varanasi, India. Contact e-mail: parimal@bhu.ac.in.

unfavorable volume ratio of metal to oxide (Ref 21-23). Corrosion and electrochemical properties, especially in contact with human body fluid where thermally oxidized metal interacts with such fluid after implantation in the body, are also reported mainly for high-temperature oxidized material (Ref 24-26). Further, limited efforts have been made in the past to establish a relationship between the thermal treatment temperatures imparted to cp-Ti with its corrosion resistance in contact with human body fluid. The deliberations on possible causes for the poor performance of higher-temperature oxidized cp-Ti are also scarcely available in the published literature. Our initial study on the influence of treatment temperature on the nature of oxides film formed on cp-Ti metal had shown that a lower treatment temperature imparts more tenacious and protective film in comparison with that formed at higher temperatures. In view of the above, it was considered important to optimize the temperature of thermal oxidation for cp-Ti to achieve an oxide film which can last longer in contact with human body fluid. In view of this, the present investigation was taken up to study the effect of thermal oxidation to improve surface properties of commercially pure titanium metal, a popular material for design and fabrication of implants, on the nature of resultant oxides and their corrosion resistance in contact with simulated human body fluid.

2. Experimental Details

The flat samples of cp-titanium ($10 \times 10 \times 2$ mm) were cut from a sheet and mechanically polished on rough to fine grades of emery papers. The final polishing was carried out on Selvyt cloth using suspension of alumina powder as abrasive ($1 \mu\text{m}$ size). The samples were subsequently cleaned with distilled water using ultrasonic cleaner and finally with acetone. Specimens in triplicate were oxidized at different temperatures (200, 300, 400, 500, 600, 700, 800 and 900 °C) for 1 h in air and cooled in furnace to room temperature.

Thermally oxidized samples were examined for the nature of oxides formed on their surfaces using different analytical techniques namely scanning electron microscopy, x-ray diffraction and Raman spectroscopy. Scanning electron microscope equipped with energy-dispersive x-ray to analyze the content of elements was used to study the morphology and elements present in the oxides film formed at different temperatures. XRD studies were performed using instrument supplied by Bruker, Germany. The cathode for x-ray radiation was $\text{Cu K}\alpha$ ($\lambda = 1.5406$ nm), with 2θ angles ranging from 10° to 80° at room temperature. Raman spectroscopy of the oxidized samples were performed by Almega Dispersive Micro-Raman spectroscope (Model Almega, by Thermo electron corporation, USA) using an exciting Nd-YAG laser beam with a wavelength of 532 nm. The lowest laser power was used (6 mW) to avoid transformation of the oxide film due to heating effects. Laser beam was focused on samples through an Olympus microscope at the magnification of 50x. The sample holder was a computer-controlled motorized platform with Jokey to provide fine focusing on desired parts of the samples. The grating was 672 lines/mm with a $25\text{-}\mu\text{m}$ pinhole. Prior to the analysis of samples, the instrument was calibrated using pure silicon with a Raman peak of 520.45 cm^{-1} . The collection time was varied between 80 and 160 s to get good peaks of the samples.

Three sets of the oxidized samples were mounted in cold setting resin to expose a surface area of 0.95 cm^2 and fitted in

cells to perform electrochemical impedance spectroscopy (EIS). The tests were conducted by exposing the samples in simulated body fluid (SBF) containing 6.5 gm/L NaCl, 0.24 gm/L CaCl_2 , 0.42 gm/L KCl and 0.2 gm/L NaHCO_3 . The pH of this solution measured at 25 °C was 7.8. SBF was preferred as the test electrolyte to assess the performance of the oxidized surfaces as this environment is closer to the actual application of the subject material intended for use. EIS experiments were performed using a Gamry made potentiostat equipped with DC 105 and CMS 300 software to analyze the data. Saturated calomel electrode (SCE) and pure graphite rod of 32 mm diameter and 150 mm length were used as reference and auxiliary electrodes. The tests were performed at open-circuit potential of the samples by imposing 10 mV of sinusoidal voltage and changing its frequency from 100 kHz to 0.01 Hz. The experiments were continued for 300 h at interval of 72 h using the same sample continuously exposed in the test solution. These sets of experiments helped to determine the minimum treatment temperature required to achieve optimum resistance to corrosion.

3. Results and Discussion

In the first part of this section, the experimental results on corrosion characteristics of cp-Ti oxidized at different temperatures will be described. The second part will incorporate the deliberations explaining the causes for improved corrosion resistance of samples thermally treated at 500 °C.

3.1 Corrosion Resistance of the Samples Oxidized at Different Temperatures

The change in open-circuit potential (E_{OCP}) of the non-oxidized and oxidized samples at different temperatures after exposure for 300 h in simulated body fluid is shown in Fig. 1. The measured E_{OCP} values for the non-oxidized and those oxidized up to 500 °C did not exhibit any appreciable change. However, a significant shift of potential took place for the sample oxidized at 600 °C. The potential of the sample oxidized at this temperature shifted about 300 mV in active direction in comparison with that of the 500 °C sample. There

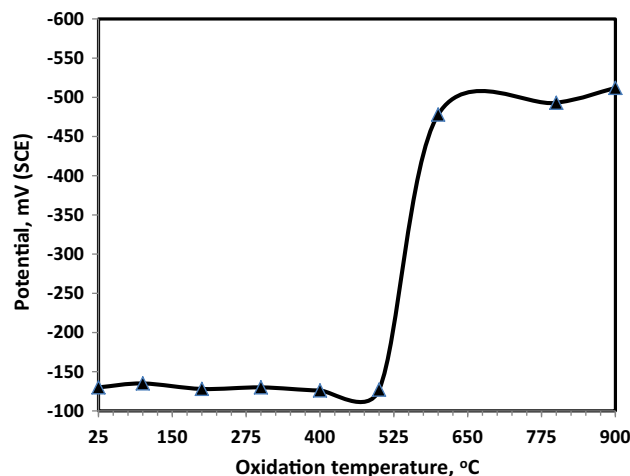


Fig. 1 Variation of open-circuit potential with oxidation temperature of cp-Ti exposed in simulated body fluid for 300 h

after it attained by and large a stable potential of around -500 mV (SCE). These results suggest that a deterioration in the protective properties of the film of cp-Ti took place above the oxidation temperature of 600 °C. It is to be noted that although the open-circuit potential does not provide any absolute value on the kinetics of metal's corrosion, it is certainly useful to understand the nature of the protective film formed on a metal surface. A shift of potential in active direction is an indication of depolarization of the anodic part of the corrosion reaction. In other words, the more surface area of the metal substrate is exposed to the electrolyte causing an augmented rate of anodic reactions (Ref 27, 28).

To have a quantitative evaluation of the corrosion resistance of the oxides formed at different temperatures, the samples were tested by electrochemical impedance spectroscopy (EIS) technique. The Nyquist plots for three samples namely untreated, 500 and 900 °C thermally treated are shown in Fig. 2 (to avoid crowding in the figure, the plots only for three samples with distinct performance are shown in this figure. Other tested samples also exhibited similar behavior). A perusal of the EIS spectra recorded for the untreated and oxidized samples shows that all the plots exhibit capacitive behavior showing about 45° intercept line with real impedance axis in Nyquist plots. This indicated that the corroding interface did not comprise simply resistance and double-layer capacitance components but also other elements were active who influenced the nature of the plots. In view of this, the data of the impedance spectra were fitted in equivalent electrical circuit incorporating constant phase element (CPE), solution resistance (RS), pore resistance (taken as the polarization resistance, R_p) and Warburg diffusion component (W), schematically shown in Fig. 3. The fitting of the data for untreated, 400 , 500 and 900 °C oxidized samples using the above equivalent circuit (Fig. 3) is shown in Fig. 4(a) and (b). It is seen from the curves of Fig. 4(a) that the fitting of the data for the log frequency-log modulus of impedance was reasonably good in all the cases. The above circuit of Fig. 3 also provided satisfactorily good fitting for the log frequency-phase shift data (4b). The fitting of the data was also performed for the other samples using the same model (plots not shown), and corresponding average electrochemical parameters extracted from the best fit results of three samples at each temperature are recorded in Table 1. The goodness of fits varied between 3.2×10^{-3} and 6.9×10^{-3} which indicate that the accuracy of the data was reasonably good for the tested samples. The polarization resistance (R_p) of the samples treated under different conditions as recorded in Table 1 reveals that the 500 °C oxidized surface exhibited considerably higher value of R_p (1.7 M Ω) than the other samples. The oxidation of cp-titanium above the temperature of 500 °C has deteriorated their corrosion resistance. The polarization resistance is inversely related to corrosion rate of a corroding interface in an electrolyte by the Stern-Geary equation:

$$I_{\text{corr}} = \frac{\beta_a \times \beta_c}{2.3(\beta_a + \beta_c) \times R_p} \quad (\text{Eq 1})$$

$$\text{Or } I_{\text{corr}} = B/R_p \quad (\text{Eq 2})$$

In the above equations, I_{cor} is corrosion current density, $B = \frac{\beta_a \times \beta_c}{2.3(\beta_a + \beta_c)}$ and β_a and β_c , respectively, are anodic and cathodic Tafel slopes of the corroding metal. Thus, higher the value of polarization resistance, lower is the corrosion rate.

The data recorded in Table 1 further reveal that the R_p values of the test specimens initially increase with their treatment temperatures, attaining a peak value at 500 °C, and then gradually have a decreasing trend with increase in temperature. These results may be attributed to the effect of oxidation on the surface of the metal samples. Untreated material had a natural thin film which was not resistant enough to withstand the corrosive effect of SBF, especially to the chloride ions present in this solution. On increasing the oxidation temperature to 400 and 500 °C, growth occurred in the film formed at ambient temperature resulting in improvement in their corrosion resistance. However, the oxidation above 500 °C caused a significant decrease in the protective properties of the oxide film. The sample treated at 500 °C attains the polarization resistance which is about 65 times and 293 times, respectively, higher than that of the untreated and 900 °C oxidized surfaces of cp-Ti. These results clearly indicate that the nature of the oxides formed on surface of the tested material by thermal oxidation plays very significant role in imparting resistance to deterioration of cp-Ti in contact with SBF.

There are some other parameters incorporated in Table 1 that need to be considered while discussing the characteristics of the corroding interface of the exposed samples and the test electrolyte. The constant phase element (CPE) denoted by Y_0 , recorded in the extreme right column of the table vary in the range of 2.17 - 23.06 μF which are of the same order as reported by the earlier researchers (Ref 29). CPE is affected due to various reasons that influence the corroding interface. Among these factors, the roughness of the surface, inhomogeneous reaction rates, thickness and porosity present in the oxide films and non-uniform distribution of current on the test surface are the main elements that influence CPE (Ref 30). Considering the components present at the corroding interface during this study, the surface roughness and porosity appear to be more appropriate ingredients than the others in changing the value of CPE. It is reported that increase in surface roughness and porosity in surface film increases the CPE component and vice versa (Ref 31, 32). The data for Y_0 are the lowest for 400 °C sample, and thereafter, it increases for higher-temperature oxidized samples. The value is significantly increased for 900 °C sample. As will be evident from the results of scanning electron microscopy described in the subsequent paragraphs, the higher-temperature oxidized samples (> 500 °C) developed greater porosity than the samples oxidized at lower temperatures.

3.2 Causes for the Improved Corrosion Resistance of Oxidized Samples at 500 °C

The superior corrosion resistance performance of 500 °C oxidized surface of cp-titanium than the other samples needs proper explanations with support of experimental and scientific evidences. In view of this, the samples were examined by scanning electron microscope and the elemental analysis was performed by energy-dispersive x-ray (EDX) analysis. EDX analysis though is not very accurate, but it certainly gives inkling about the concentration of the elements present in a material. The accuracy of the EDX analysis was ascertained by recording the analysis data minimum at three locations of the samples. The concentration at different locations did not vary to a considerable extent. The average of three analysis results was taken and is recorded microphotographs. The scanning electron

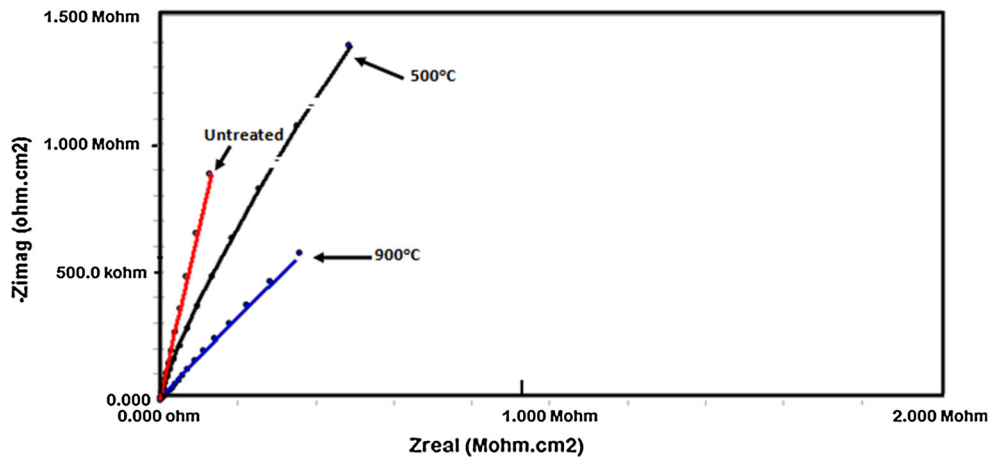


Fig. 2 Nyquist impedance plots for untreated and thermally oxidized samples

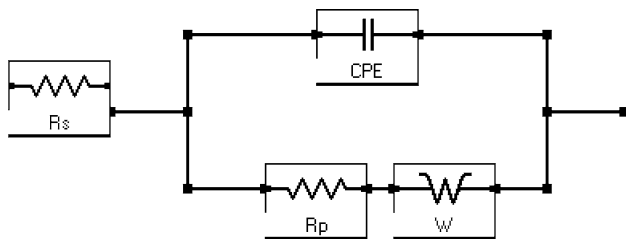


Fig. 3 Equivalent electrical circuit of simplex model incorporating constant phase element (CPE) and Warburg diffusion component (W); R_p and R_s are polarization resistance and solution resistance, respectively

microphotographs (with % concentration of Ti and oxygen determined by energy-dispersive x-ray analysis and printed at the bottom of the left side of the photographs) of the samples oxidized at different temperatures are shown in Fig. 5(a-i). It is seen that oxygen is present on the surface of all the samples, of course with varying concentration from 16 to 41%. This indicates that oxides of titanium were present on the surfaces of each of the samples. Further, the concentration of oxygen on the samples, untreated and oxidized at 200, 300 and 400 °C are approximately constant (varying from 16 to 21%). These results indicate that similar types of oxides were present on the surfaces of these samples. An increase in oxygen concentration is recorded at the surface of the samples oxidized at 500 °C and above, indicating either change in the phase of oxides or increase in the proportion of oxides with higher content of oxygen. Among the various known oxides of titanium, TiO_2 incorporates the highest concentration of oxygen. Considering the results of EDX analysis of about 16 to 21% oxygen present in the untreated and the samples oxidized up to 400 °C, none of the oxides of titanium can be attributed to this concentration of oxygen. It is reported that cp-titanium forms non-stoichiometric and amorphous titanium oxide layer of about 3-7 nm thick at room temperature which protects the metal from corrosion (Ref 33-35). Based on the EDX analysis data where oxygen content in the oxide was recorded in the range of 16-21%, it was not appropriate to assign any specific phase of titanium oxide for these conditions.

A gradual increase in concentration of oxygen in the oxide formed at 500 °C and above (Fig. 4e-i) was recorded. The morphology of the film present on the samples oxidized at and

above 500 °C also showed remarkable changes. The oxygen concentration in the range of 30-40% noted for 500, 600 and 900 °C samples indicated the presence of the phases of TiO_2 on the surface of these samples.

The morphologies of the oxide particles on the untreated sample and those oxidized at 200 °C/300 °C appear spherical with approximate particle size of <10 nm. The morphology changed on the samples oxidized at 400 °C and above. Also the crystallite size is noted to increase in samples oxidized at and above 400 °C (Fig. 5d-i). A very sharp increase in crystallite sizes took place in the samples oxidized at 800 and 900 °C where the sizes ranged between 800 and 1000 nm. The increased crystallite size with temperature is attributed to increased rate of crystallization at higher temperatures (Ref 36, 37). Another notable observation from these figures is an increasing trend in porosity of the oxide film with increase in oxidation temperature.

The above results suggest that the samples oxidized above 500 °C developed oxide film having higher crystallite size and porosity. These changes probably deteriorated the protective nature of the film formed on the surface of cp-Ti as noted above during the assessment of their resistance to corrosion in simulated body fluid (Table 1).

The EIS and SEM/EDXA results as described above indicate that the surface of cp-Ti formed various types of oxides at different oxidation temperatures which significantly changed their morphology and corrosion resistance. In view of this, the oxide phases formed on the surface of the studied samples were examined by XRD and Raman spectroscopy. XRD pattern of surface films formed at different temperatures is shown in Fig. 6. It may be seen that peaks of different oxide phases of titanium are recorded on the surface of all the studied samples. The peaks of titanium sesquioxide (tistarite, Ti_2O_3) and anatase (TiO_2) are noted on the untreated and the samples oxidized at 200, 300, 400 and 500 °C. At the oxidation temperatures of 600, 700 and 800 °C, the peaks of Ti_2O_3 are vanished and phases of rutile (TiO_2) and Ti_3O (titanium oxide) with increased intensity of peaks of rutile are recorded. At 900 °C, the whole surface is transformed into rutile phase of TiO_2 . This observation is in conformity with the findings of the other researchers (Ref 21, 23). It is reported that cp-Ti oxidized at lower temperatures forms the film comprising of anatase and Ti_2O_3 (Ref 38, 39). The absence of the phase of anatase in XRD patterns of the untreated and other samples may be due to its amorphous nature.

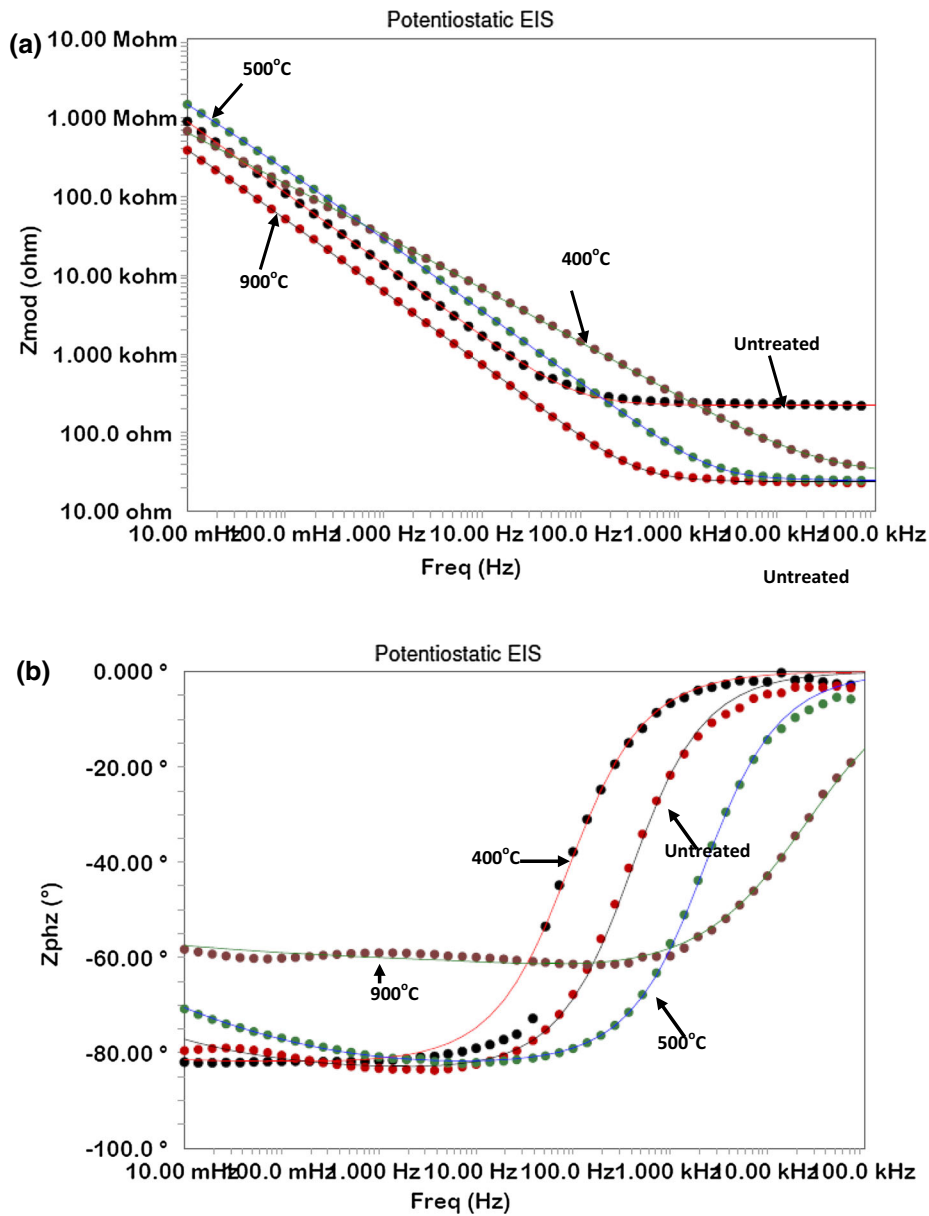


Fig. 4 (a) Potentiostatic EIS Bode Zmod vs. frequency plots for untreated, 400, 500 and 900 °C oxidized samples after 300 h of their exposure in Ringer's solution; symbols on the plots are experimental data and solid lines are after fitting the data. (b) EIS log frequency-phase Bode plots for untreated, 400, 500 and 900 °C oxidized samples after 300 h of their exposure in Ringer's solution; symbols on the plots are experimental data and solid lines are after fitting the data

Table 1 Electrochemical parameters extracted from the EIS plots of oxidized surface of cp-titanium

Oxidation temperature, °C	Electrochemical parameters			
	R_{us}, Ω	$R_p, M\Omega \text{ cm}^2$	α	$Y_0, S^*s^\alpha \times 10^{-6}$
25	22	0.026	0.913	13.79
400	21	0.174	0.860	2.17
500	25	1.70	0.914	2.37
600	39	0.009	0.890	6.47
700	28	0.004	0.703	7.61
800	16	0.0051	0.843	17.5
900	24	0.0058	0.543	23.06

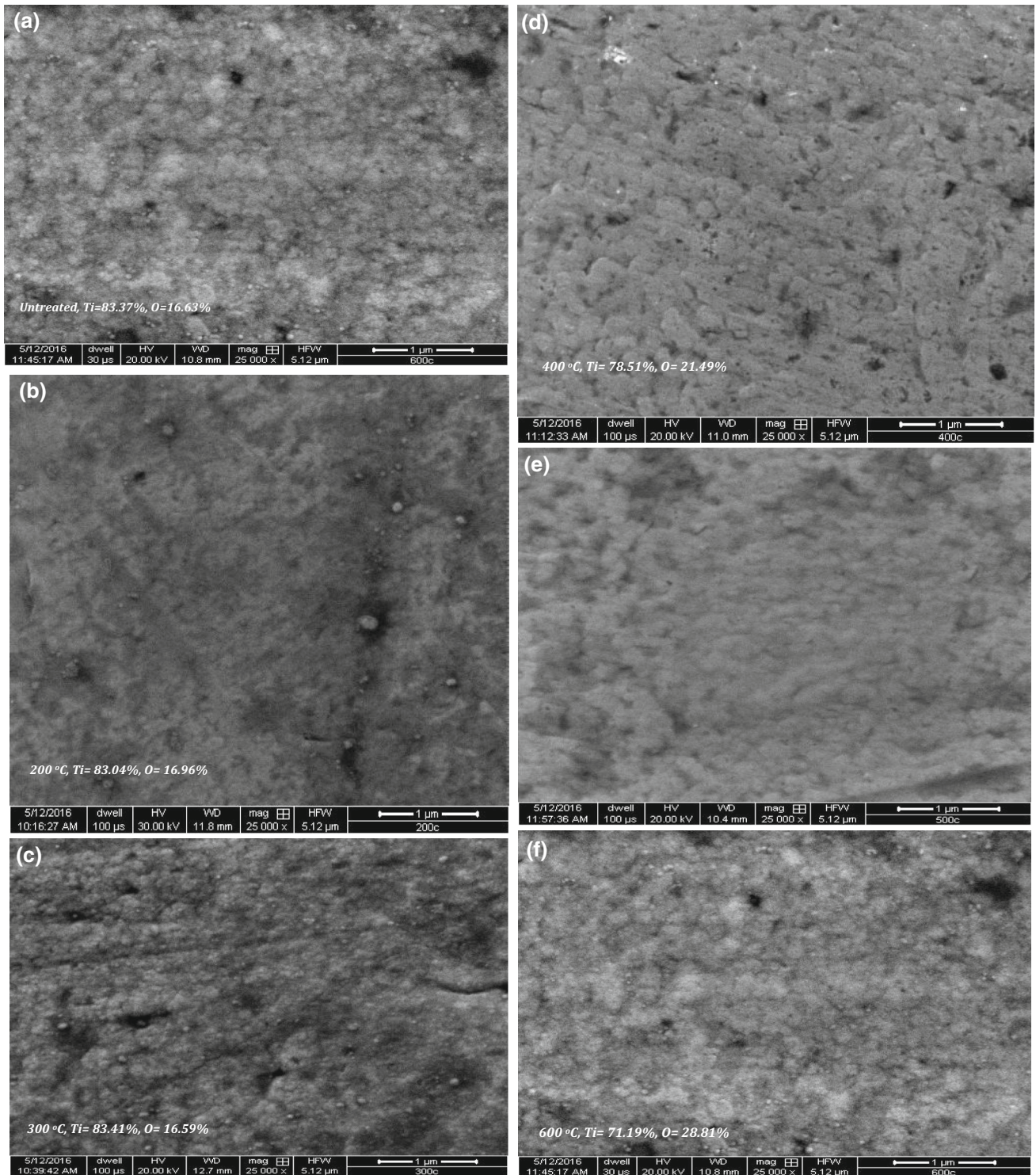


Fig. 5 Morphology of the oxides film formed at (a) untreated; (b) 200 °C; (c) 300 °C; (d) 400 °C; (e) 500 °C; (f) 600 °C; (g) 700 °C; (h) 800 °C and (i) 900 °C

To probe the samples further, they were subjected to Raman spectroscopy and the resultant spectra are shown in Fig. 7(a-c). It may be seen from the spectra of the untreated and lower temperature oxidized samples (200, 300, 400 and 500 °C) that this technique yielded peaks of anatase and aristite (Ti_2O_3), though a bit weak in intensity. Corresponding peaks for these phases of oxides are shown in Fig. 7(a) and (b). The Raman

peaks of rutile observed on the samples oxidized at 500 and 600 °C (at 610 and 446 cm^{-1}) are also present in the 700-900 °C oxidized samples. It is to be noted that the Ti_3O phase which was detected in XRD pattern of oxides of 600, 700 and 800 °C did not appear in Raman spectra of these samples. Literature search revealed that this phase of oxide of titanium is Raman inactive (Ref 40).

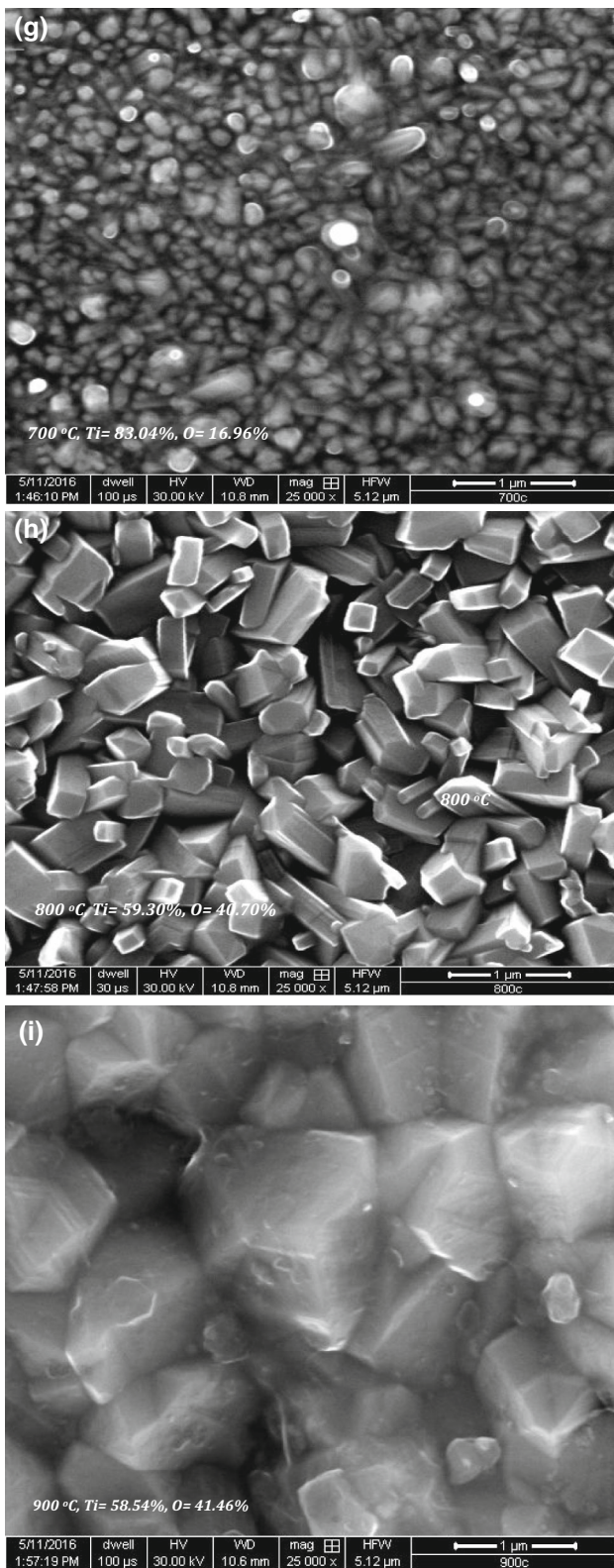


Fig. 5 continued

The confirmation of anatase form of TiO_2 by Raman spectroscopy on the untreated surface and on the samples oxidized at 200, 300 and 400 °C, but inability of XRD to identify this phase indicates that the anatase form of oxide was

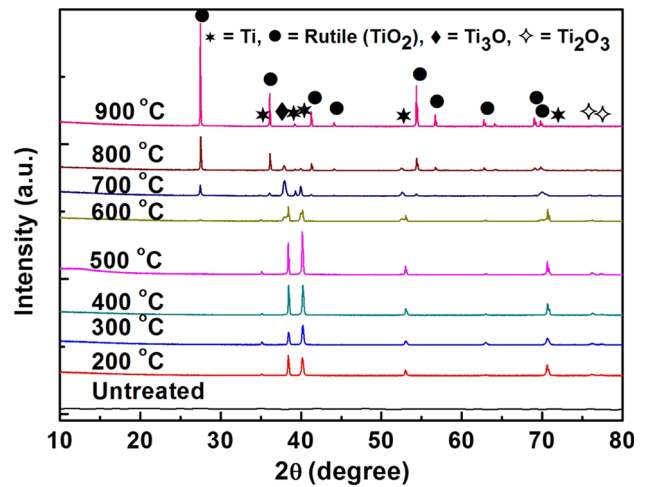


Fig. 6 XRD of surface of Cp-Ti in untreated condition and oxidized at different temperatures. The weak peaks present in untreated material are not visible and are suppressed due to the higher intensity peaks of the other samples

in its amorphous phase under these conditions. At 500 °C, a new phase (rutile, TiO_2) in addition to Ti_2O_3 and anatase emerged as evident from the XRD patterns (Fig. 6) and Raman spectra (Fig. 7b). On further increase of temperature, the latter two phases of oxides disappeared and only the phase of rutile is visible on the surface of the higher-temperature oxidized samples (Fig. 6, 7b and c). A comparison of these results with that of the impedance values recorded in Table 1 brings out very interesting correlation between the treatment temperature (and hence the development of the oxide phases) and corrosion resistance of the treated surface in contact with SBF. It may be concluded from the results recorded in Fig. 6, 7(b) and (c) and Table 1 that a combination of the phases of Ti_2O_3 (titanium sesquioxide), anatase and rutile formed on the surface of 500 °C sample was the most effective in increasing its corrosion resistance. The higher oxidation temperatures, which resulted in the transformation of anatase and Ti_2O_3 into the single phase of rutile (Fig. 6 and 7(b) and c), caused a substantial reduction in resistance to corrosion of the tested materials. These observations suggest that a composite film of oxides (Ti_2O_3 , anatase and rutile) formed on the surface of the sample oxidized at 500 °C resulted in an improvement in the corrosion resistance of these samples.

To see the compactness of the formed oxides, the interfaces of 500 and 900 °C samples were examined and the microphotographs are shown in Fig. 8. It is evident from the figure that an intact interface between the substrate and oxide without any defect is present in 500 °C sample, whereas 900 °C oxidized material exhibits a broken interface geometry with gap ranging from a few micrometer to some nanometer between the substrate and oxide. Due to a substantial difference in thermodynamical stability of the cp-Ti (substrate) and its oxides (here rutile), there is possibility of formation of potent galvanic couples; with rutile phase acting as cathode and the base titanium as anode, in the 900 °C sample. The galvanic potential developed in the presence of the SBF as electrolyte is possibly the driving force for accelerated rate of corrosion for 900 °C oxidized sample.

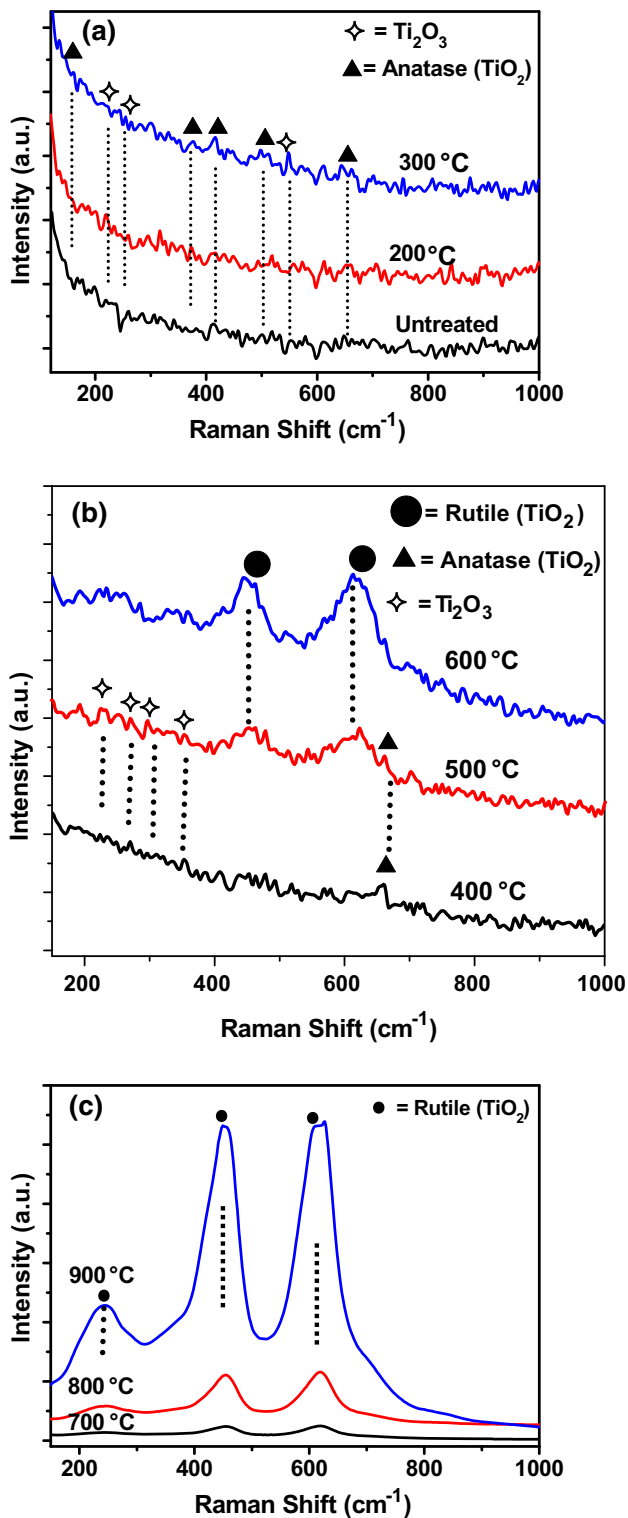


Fig. 7 Raman spectra of oxidized samples at: (a) untreated, 200, 300 °C; (b) 400, 500, 600 °C; (c) 700, 800, 900 °C

4. Conclusion

All experimental evidences show that corrosion resistance of cp-Ti can be effectively improved by thermally oxidizing its surface at 500 °C. Raman spectroscopy and XRD results show that at this oxidation temperature the surface oxide of the metal

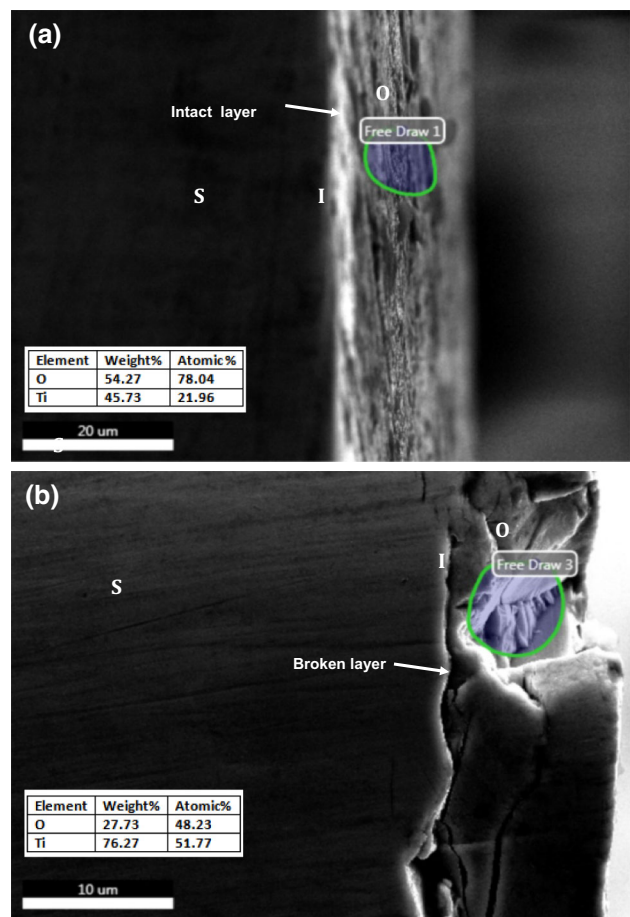


Fig. 8 Scanning electron microphotographs and EDX analysis of oxide-substrate interface of the samples oxidized at (a) 500 °C and (b) 900 °C. The letters S, I and O, respectively, denote substrate, interface and oxide zones

is transformed into the composite phases of anatase, Ti₂O₃ and rutile. At higher temperature of oxidation (600-800 °C), the nature of the oxide film on the metal surface was completely transformed into rutile (TiO₂) and Ti₃O (titanium oxide). At 900 °C, whole surface oxidized into rutile with significant coarsening effect on oxide particles. These changes resulted in degradation of corrosion resistance of the higher-temperature oxidized samples. The results further show that the deterioration of the sample oxidized at 900 °C was caused due to the formation of pores at the interface of substrate and oxide layer. The interface of the 500 °C sample, on the other hand, had an intact layer.

References

1. M. Balazic, J. Kopac, M.J. Jackson, and W. Ahmed, Review: Titanium and Titanium Alloy Applications in Medicine, *Int. J. Nano Biomater.*, 2007, **1**, p 3-34
2. M. Niinomi, Mechanical Bio Compatibilities of Titanium Alloys for Biomedical Applications, *J. Mech. Behav. Biomed. Mater.*, 2007, **1**, p 30-42
3. J.E. Lemons, Biomaterials, Biomechanics, Tissue Healing and Immediate Function Dental Implants, *J. Oral implantol.*, 2003, **30**, p 318-324

4. C.E. Misch, J.T. Strong, M.W. Bidez, in *Scientific Rationale for Dental Implant Design: Contemporary Implant Dentistry*, ed. by C.E. Misch, Chapter 11, (St Luis, Mosby, 2008), pp. 200–229
5. S. Kumar, T.S.N. Narayanan, S.G. Raman, and S.K. Seshadri, Thermal Oxidation of CP-Ti: Evaluation of Characteristics and Corrosion Resistance as a Function of Treatment Time, *Mater. Sci. Eng. C*, 2009, **29**, p 1942–1949
6. J.E. Sundgren, P. Bodo, and I. Lundstrom, Auger Electron Microscopic Studies of the Interface Between Human Tissue and Implants Of Titanium and Stainless Steel, *J. Colloid Interface Sci.*, 1984, **110**, p 9–20
7. C.J. Goodacre, G. Bernal, K. Rungcharassaeng, and J.Y. Kan, Clinical Complications with Implant and Implant Prosthesis, *J. Prosthet. Dent.*, 2003, **90**, p 121–132
8. L.H. Li, Y.M. Kong, H.W. Kim, Y.W. Kim, H.E. Kim, S.J. Heo, and J.Y. Koak, Improved Biological Performance of Ti Implants Due to Surface Modification by Micro-arc Oxidation, *Biomaterials*, 2004, **25**, p 2867–2875
9. Y.T. Sul, C. Johansson, A. Wennerberg, L.R. Cho, B.S. Chang, and T. Albrektsson, Optimum Surface Properties of Oxidized Implants for Reinforcement of Osseointegration: Surface Chemistry, Oxide Thickness, Porosity, Roughness and Crystal Structure, *Int. J. Oral Maxillofac. Implants*, 2005, **20**, p 349–395
10. M. Wen, C. Wen, P. Hodgson, and Y. Li, Improvement of the Biomedical Properties of Titanium Using SMAT and Thermal Oxidation, *Colloids Surf. B Biointerfaces*, 2014, **116**, p 658–665
11. Y.H. Huang, A.V. Xiropoulos, R.G. Sorensen, J.M. Albandar, J. Hall, and U.M. Wikesjo, Bone Formation at Titanium Porous Oxide (TiUnite) Oral Implants in Type IV Bone, *Clin. Oral Implants Res.*, 2005, **16**, p 105–111
12. H. Guleryuz and H. Cimenoglu, Effect of Thermal Oxidation on Corrosion and Corrosion-Wear Behaviour of a Ti-6Al-4V Alloy, *Biomaterials*, 2004, **25**, p 3325–3333
13. H. Guleryuz and H. Cimenoglu, Surface Modification of a Ti-6Al-4V Alloy by Thermal Oxidation, *Surf. Coat. Technol.*, 2005, **192**, p 164–170
14. E. Gemelli, A. Scariot, N. Heriberto, and A. Camargo, Thermal Characterization of Commercially Pure Titanium for Dental Applications, *Mater. Res.*, 2007, **10**, p 241–246
15. B. Feng, J.Y. Chen, S.K. Qi, L. He, J.Z. Zhao, and X.D. Zhang, Characterization of Surface Oxide Films on Titanium and Bioactivity, *J. Mater. Sci. Mater. Med.*, 2002, **13**, p 457–464
16. E. Gemelli and N.H.A. Camargo, Oxidation Kinetics of Commercially Pure Titanium, *Revista Matéria*, 2007, **12**, p 525–531
17. S. Kumar, T.S.N. Sankara Narayanan, S.G. Sundara Raman, and S.K. Seshadri, Thermal Oxidation of CP Ti- an Electrochemical and Structural Characterization, *Mater. Charact.*, 2010, **61**, p 589–597
18. B.B. Zhang, B.L. Wang, L. Li, and Y.F. Zheng, Corrosion Behaviour of Ti5Ag Alloy with and Without Thermal Oxidation in Artificial Saliva Solution, *Dent. Mater.*, 2011, **27**, p 214–220
19. M. Jamesh, T.S.N. Sankara Narayanan, and P.K. Chu, Thermal Oxidation of Titanium: Evaluation of Corrosion Resistance as a Function of Cooling Rate, *Mater. Chem. Phys.*, 2013, **138**, p 565–572
20. J. Hu, Y. Wang, and D.Y. Wang, Thermal Oxidation of CP-Ti at Different Temperatures, *Adv. Mater. Res.*, 2010, **146-147**, p 1536–1539
21. A. Bloyce, Z. Qi-Y, H. Dong, and T. Bell, Surface Modification of Titanium Alloys for Combined Improvements in Corrosion and Wear Resistance, *Surf. Coat. Technol.*, 1998, **107**, p 125–132
22. H. Dong, A. Bloyce, P.H. Morton, T. Bell, in *Titanium 1995. Science and Technology*, ed. by P.A. Blenkinsop, W.J. Evans, vol. II (Institute of Materials, London, 1996), pp. 1999–2006
23. G.P. Burns, Titanium dioxide dielectric films formed by rapid thermal oxidation, *J. Appl. Phys.*, 1989, **65**, p 2095–2097
24. J.E.G. Gonzalez and J.C. Mirza-Rosca, Study of the Corrosion Behavior of Titanium and Some of Its Alloys for Biomedical and Dental Implant Applications, *J. Electroanal. Chem.*, 1999, **471**, p 109–115
25. P. Kofstad, *High Temperature Corrosion* (Elsevier Applied Science, Essex, 1988)
26. M.A. Khan, R.L. Williams, and D.F. Williams, Conjoint Corrosion and Wear in Titanium Alloys, *Biomaterials*, 1999, **20**, p 765–772
27. M.G. Fontana, *Corrosion Engineering*, 3rd ed., McGraw-Hill, New York, 1997
28. G.W. Reade, C. Kerr, B.D. Barker, and F.C. Walsh, The importance of substrate surface condition in controlling the porosity of electroless nickel deposits, *Trans. Inst. Met. Finish.*, 1998, **76**, p 149
29. Nianwei Dai, Lai-Chang Zhang, Junxi Zhang, Qimeng Chena, and Wu Maoliang, Corrosion Behavior of Selective Laser Melted Ti-6Al-4V Alloy in NaCl Solution, *Corros. Sci.*, 2016, **102**, p 484–489
30. J.R. Macdonald, *Impedance Spectroscopy*, Wiley, New York, 1987
31. A. Toloei, V. Stoilov, D. Northwood, The relationship between surface roughness and corrosion, in *Proceedings of the ASME 2013 International Mechanical Engineering Congress & Exposition, IMECE2013*, November 13–21, 2013, San Diego, California, USA. www.researchgate.net/publication/267596825
32. A.S. Toloei, V. Stoilov, D.O. Northwood, Simultaneous effect of surface roughness and passivity on corrosion resistance of metals. *Materials Characterization VII 355*, WIT Transactions on Engineering Sciences, Vol 90, © 2015 WIT Press, www.witpress.com, ISSN 1743-3533 (on-line)
33. D.M. Brunette, P. Tengvall, M. Textor, and P. Thomsen, *Titanium in Medicine*, Springer, New York, 2001
34. S.G. Steinemann, Titanium—the Material of Choice?, *Periodontology*, 1998, **2000(17)**, p 7–21
35. M. Zhou, J. Yu, S. Liu, P. Zhai, and L. Jiang, Effects of Calcination Temperatures on Photocatalytic Activity of SnO₂/TiO₂ Composite Films Prepared by an EPD Method, *J. Hazard. Mater.*, 2008, **154**, p 1141–1148
36. S. Shao, M. Dimitrov, N. Guan, and R. Kohn, Crystalline Nanoporous Metal Oxide Thin Films by Post-Synthetic Hydrothermal Transformation: SnO₂ and TiO₂, *Nanoscale*, 2010, **2**, p 2054–2057
37. S. Takenaka, R. Takahashi, S. Sato, T. Sodesawa, F. Matsumoto, and S. Yoshida, Pore Size Control of Mesoporous SnO₂ Prepared by Using Stearic Acid, *Microporous Mater.*, 2003, **59**, p 123–131
38. X. Cheng and S.G. Roscae, Corrosion Behaviour of Titanium in the Presence of Calcium Phosphate and Serum Proteins, *Biomaterials*, 2005, **26**, p 7350–7356
39. J. Pouilleau, D. Devilliers, F. Garrido, S. Durand-Vidal, and E. Mahe, Structure and Composition of Passive Titanium Oxide Film, *Mater. Sci. Eng. B*, 1997, **47**, p 235–243
40. P. Thakur, B. Tan, and K. Venkatakrisnan, Multi-phase Fictionalization of Titanium for Enhanced Photon Absorption in the Vis-NIR Region, *Sci. Rep.*, 2015, **5**, p 15354. doi:10.1038/srep15354